Iraqi National Journal of Earth Science

www.earth.mosuljournals.com

Petrography and Geochemistry of Dolerite Exotic Rocks at Sanam Salt Dome, Southern Iraq

Ghufran Basil Ghayadh [1], Sattar J. Al-Khafaji [2*]

[1,2] *Department of Geology, College of Science, University of Basrah, Basrah, Iraq.*

Article information

Received: 05- Jun-2024

Revised: 03- Aug-2024

Accepted: 07- Nov -2024

Available online: 01- Oct – 2025

Keywords:
Dolerite
Basaltic andesite
Hydrothermal alteration
Sanam salt dome
REE

Correspondence:
Name: Sattar J. Al-Khafaji

Email: Khafaji52000@gmail.com

ABSTRACT

Four samples of dolerite rocks are selected to conduct their petrography and geochemical properties. Dolerite rocks exist as large blocks and fragments exposed in the southeastern part of the Sanam salt dome, Basrah, Iraq. The petrography reveals that their characteristic ophitic texture is dominant. Anorthite and augite are the main minerals of dolerite, whereas hornblende, quartz, chlorite, sericite, and epidote are secondary minerals formed as a result of chloritization, sericitization, and epidotization, due to low-grade hydrothermal alteration. The presence of hematite in some samples reflects the oxidization condition and high oxygen activity during the late alteration processes. The major geochemical analysis shows that the studied dolerite rocks are of saturated and oversaturated basalt-type, where the composition ranges from basaltic andesite to basaltic trachyandesite, falling in both alkaline and tholeiitic basalt fields. It is worth noting that the high percentage of L.O.I, as well as relatively high silica content, indicate that the dolerite rocks have been affected by low-grade hydrothermal alteration. This is associated with metasomatism followed by weathering processes. The pattern of REE in the studied dolerite rocks, combined with other chemical analyses, suggests that the present dolerite rocks are of within-plate tholeiites.

DOI: 10.33899/earth.2024.150535.1295, ©Authors, 2025, College of Science, University of Mosul.

صخارية وجيوكيميائية صخور الدولرايت الغريبة في قبة سنام الملحية، جنوبي العراق

غفران باسل غياظ [1] ، ستار جبار الخفاجي [*2]

[2،1] قسم علوم الارض، كلية العلوم، جامعة البصرة، البصرة، العراق.

معلومات الارشفة

تاريخ الاستلام: 05- يونيو -2024

تاريخ المراجعة: 03- اغسطس -2024

تاريخ القبـول: 07- نوفمبر-2024

تاريخ النشر الالكتروني: 01- اكتوبر -2025

الكلمات المفتاحية:

دوليرايت

انديزايت البازلتي

التغيرات الحرمائية

قبة سنام الملحية

العناصر الأرضية النادرة

المراسلة:

الاسم: ستار جبار الخفاجي

Email: Khafaji52000@gmail.com

الملخص

تم اختيار أربع عينات من صخور الدولرايت في قبة سنام لمعرفة خصائصها الصخرية والجيوكيميائية. توجد صخور الدولرايت على شكل كتل وقطع كبيرة تظهر في الجزء الجنوبي الشرقي من القبة الملحية في البصرة، العراق. اظهرت الدراسة الصخرية الى ان النسيج الأوفيتي المميز لها هو النسيج السائد في الدولرايت، وان الأنورثايت والاوجايت هما المعدنان الرئيسيان للدولرايت، في حين كانت معادن الهورنبلند والكوارتز والكلورايت والسيريسايت والايبيدوت هي المعادن الثانوية التي تكونت بفعل عمليات الكلورة والسرستة والأبدتة كنتيجة لعمليات التغيير الحرمائي منخفض الحرارة. يشير وجود الهيماتايت في بعض العينات الى ظروف مؤكسِدة عالية الفعالية أثناء عمليات التغيير اللاحقة. اظهر التحليل الجيوكيميائي للعناصر الرئيسة ان صخور الدولرايت المدروسة هي عبارة عن بازلت مشبع وفوق المشبع تراوح في تركيبه من الانديسايت البازلتي الى تراخي- انديسايت البازلتي ويقع في حقل البازلت القلوي والثولييتي. ان النسبة العالية لمفقودات الحرق وكذلك المحتوى العالي نسبيا من السيليكا يشير الى ان الصخور قد تأثرت بالتغيير الحرمائي منخفض الحرارة. وقد ارتبط هذا بالتحول الذي اعقبته عمليات التجوية. يشير نمط توزيع العناصر الأرضية النادرة في صخور الدولرايت الحالية المدروسة جنبا الى جنب مع التحليلات الكيميائية الاخرى الى ان صخور الدولرايت الحالية موجودة ضمن صفائح الثولييايت.

DOI: 10.33899/earth.2024.150535.1295,

Introduction

Dolerite is a type of mafic rock that constitutes a part of the igneous oceanic crust (Wang and Davis, 2003). Dolerite rocks of the Sanam salt dome have been described in terms of petrography and mineralogy by previous researchers (Soltan, 2002, 2020; Al-Mudafar, 2019). These rocks crop out as large blocks and fragments, especially in the southeastern parts of the Sanam salt dome, as a result of the segmentation of large dykes or veins due to deformation associated with the evolution of the Sanam salt plug (Soltan, 2002, 2020). The exposed rocks of the Sanam salt dome consist of a heterogeneous mixture of rafts and boulders of various lithological composition, including dolomite, limestone igneous rocks, embedded in gypsum and or/ anhydrite matrix (Al-Naqib, 1970). There is no known geochemical investigation carried out on Sanam dolerite except Al-Bassam (2011), who conducted a chemical study on two samples of highly magnesium igneous rocks. So, this work focuses on the petrography and geochemistry of Sanam dolerite in order to present preliminary information about their composition and origin.

Geological setting and study area

The study area (Sanam salt dome) is located at latitude 30 °08′ 00" N and longitude 47° 37′ 00 " E, in Basra Governorate, about 45 Km southwest of Basrah City and 8 Km west of Safwan town near the Iraqi-Kuwait Borders. It is situated within Dibdiba Plain, southern Iraq, which belongs to the Mesopotamian zone within the unstable shelf (Buday & Jassim, 1987). Sanam is a salt dome structure composed of sedimentary, igneous, and metamorphic rocks intruded within evaporite rocks (Al-Ali *et al.*, 2022). These rocks were subjected to varied geological processes of different degrees that affected their original rock characteristic, such as diagenesis, metamorphism, deformation, and dissolution processes (Soltan, 2020). These lithologies belong to the Hormuz Series. In the Arabian Gulf region, whose age is estimated to be Infra-Cambrian (Al-Bassam, 2011). The Dibdiba sediments consist of mixed gypsum, mud, sand, and gravel overlain by 1-3 m of gypcrete overburden that covers the area around the Sanam dome (Al-Ali and Al-Khafaji, 2023). The exposed rocks of the Sanam dome form a complex component cap rock, which is usually the upper part of the salt cylindrical body that often consists mainly of evaporite (Billings, 1972). The cap rocks do not take the form of one regular dome; the layers tilt away from its top, forming a group of parasitic domes clustered together, giving the dome a semi-oval shape. The length of the long axis of the dome is 1.7 km extending NW-SE, while the short axis is 1.2 km extending NE-SW (Al-Muttory, 2002).

Materials and methods

Four samples of exotic dolerite rocks are collected from the southeastern part of the Sanam salt dome (Fig. 1). GPS type: (Garmin GPS Map 64s is used to report the location of the samples. Four thin sections for dolerite rocks have been prepared at the University of Tehran laboratory. Petrographic studies are conducted using an OPTIKA polarizing microscope in the laboratories of the Geology Department, College of Science, University of Basrah. The X-Ray Diffraction technique (PW3830 X-ray generator) is utilized to identify the mineral content of dolerites in the laboratories of Tehran University, Tehran. The XRF technique type Philips, PW 24004, is used to determine major oxides, and the ICP-MS technique type Elan DRC-E is used to determine trace elements and REEs in the laboratories of Tehran University.

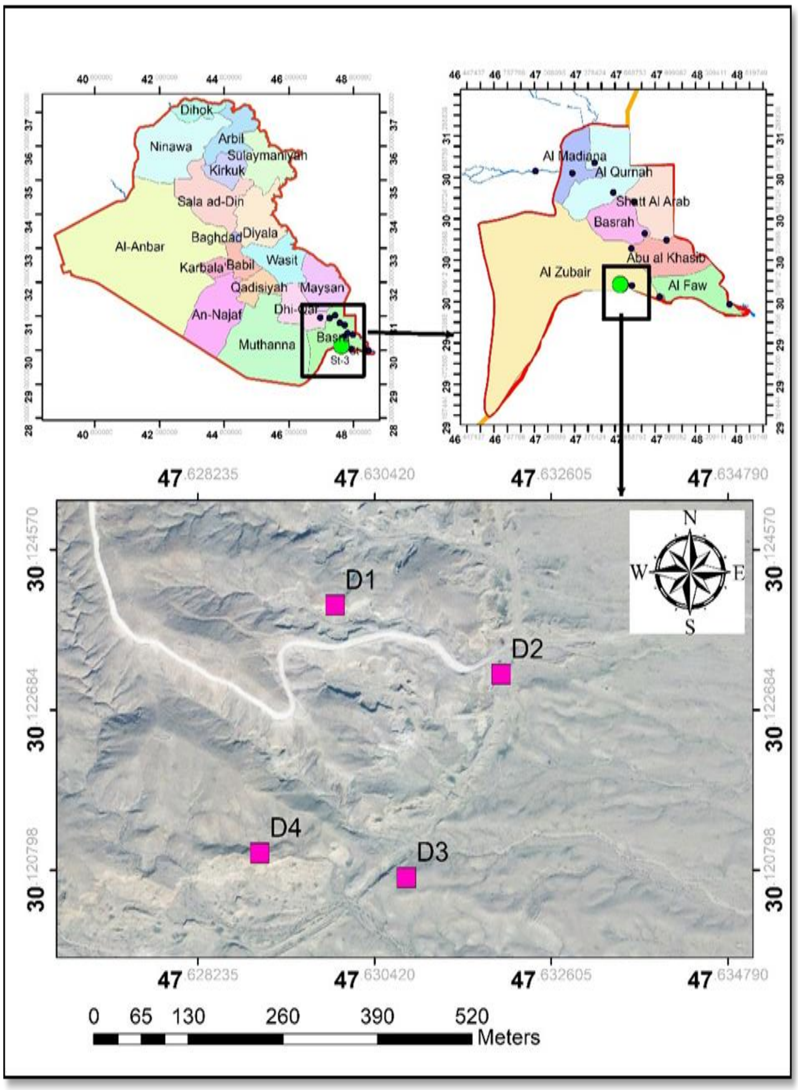

Fig. 1. Location of the study area and samples.

Results and Discussion

Results

1. Petrography and Mineralogy

Petrographical examination and mineralogical analysis of dolerite samples are conducted to determine the relationship between mineralogy and their basic geochemistry within a given system. Thus, aided in formulating an idea about the degree of alteration and weathering that occurred on the rocks.

The present mafic rocks typically exhibit their characteristic ophitic texture, that mainly composed of plagioclase (anorthite) and clinopyroxene (augite) as primary minerals. The existence of quartz, chlorite, hematite, and hornblende is considered here as a result of secondary processes. Hydrothermal alteration, as a secondary process, affected the rocks, leading to chloritization, epidotization, and sericitization of the primary igneous minerals (Plates 1a, b, c, d, e, f; Plate 2e). It is obvious from Table 1 that metasomatism, due to hydrothermal alteration, has affected the rocks. This is shown by the high SiO_2 content of the rocks that makes them fall within the range of intermediate rocks rather than the basic ones (Fig. 3). Chloritization is frequently encountered in pyroxene phenocrysts, sericite after plagioclase, and subhedral opaque minerals are most frequently observed. The assemblage of chlorite and epidote is especially observed in some thin sections as an indicator of low-grade hydrothermal alteration.

Four types of alteration are detected: chloritization, sericitization, epidotization, and silicic alteration. Chloritization of mafic minerals had led to the replacement of mafic minerals by chlorite, which gave the samples a green hue under plane-polarized light. Sericitization has altered plagioclase mineral to sericite, whereas silica, as a by-product (due to hydrothermal alterations), appears as quartz veins and interstitial hydrothermal quartz grains (Plate 2a, b). The presence of these mineral assemblages is also verified by XRD analysis (Fig. 2).

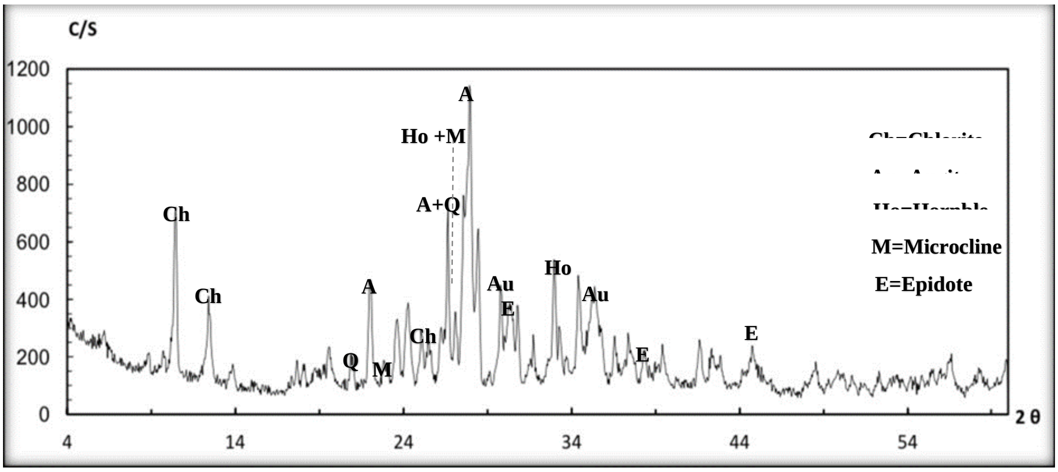

Fig. 2. X-ray diffractogram of sample D4 from Sanam Salt dome.

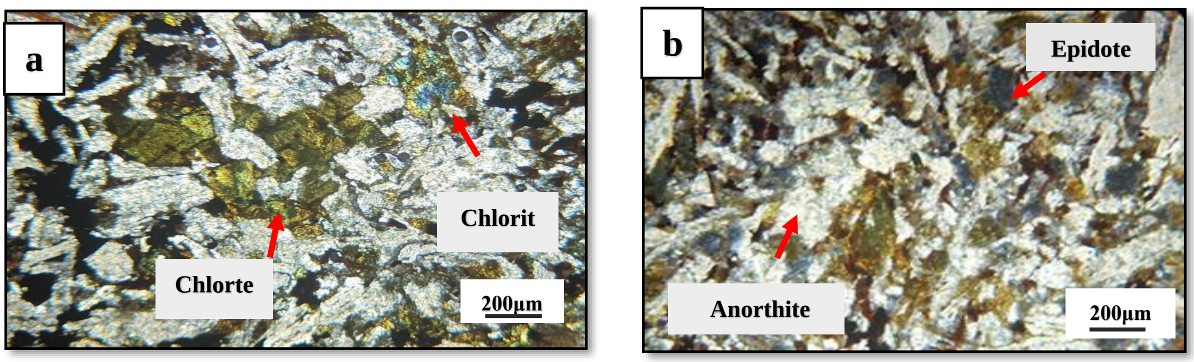

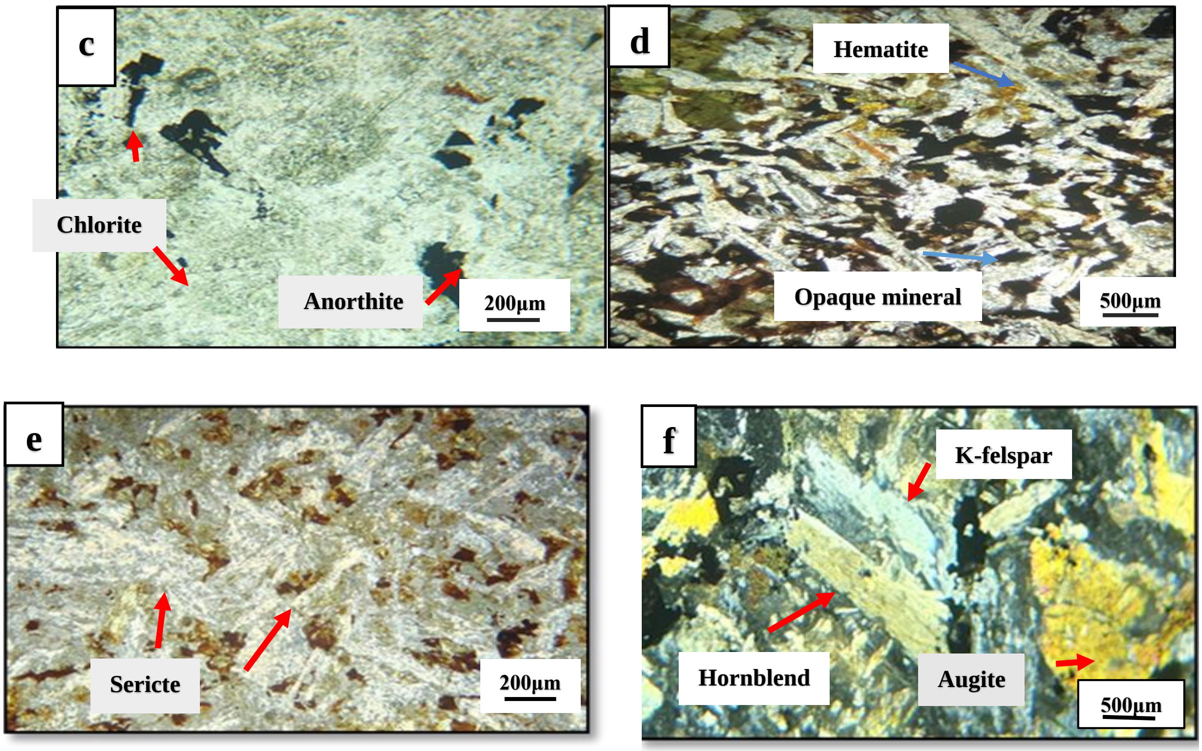

Plate 1: Photomicrographs showing the mineralogical and textural constituents of dolerite rocks a) Chlorite mineral in D3 [XPL], b) Plagioclase and epidote minerals in D3 [XPL], C) Chlorite and plagioclase mineral in D3 [XPL], d) Hematite and opaque mineral in D4 [PPL], e) Sericite mineral in D2 [XPL], f) Hornblende and K-feldspar mineral in D4 [XPL].

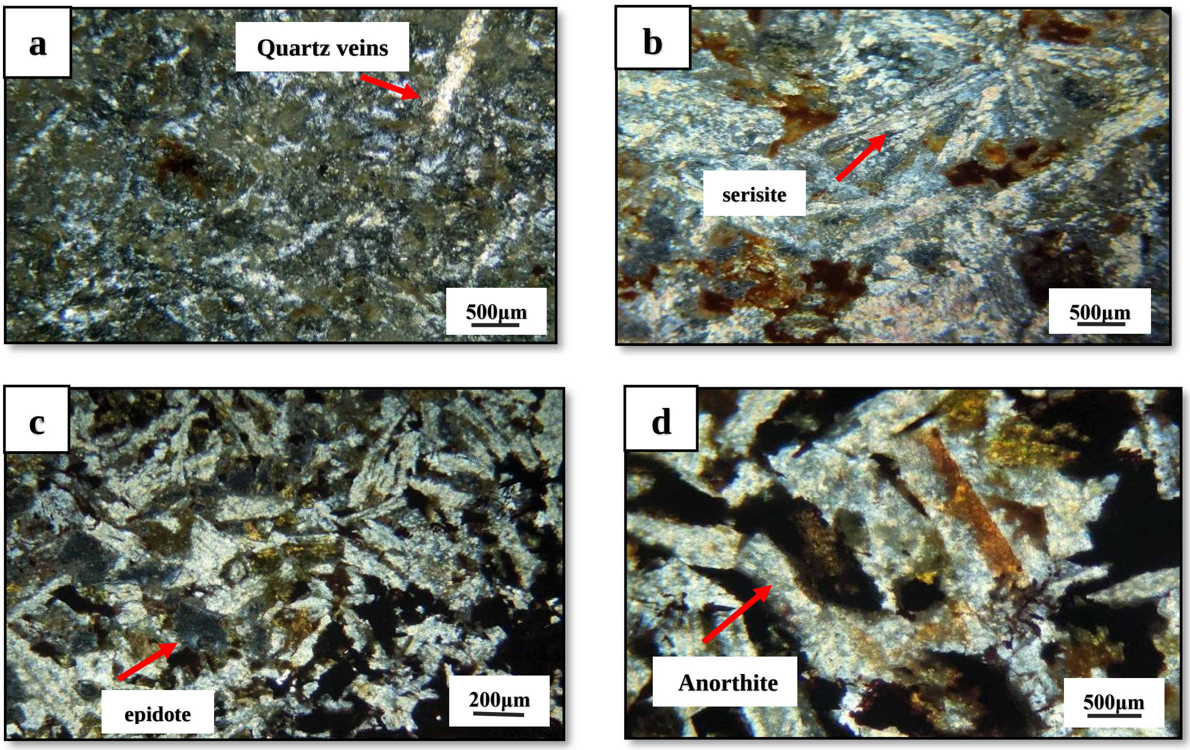

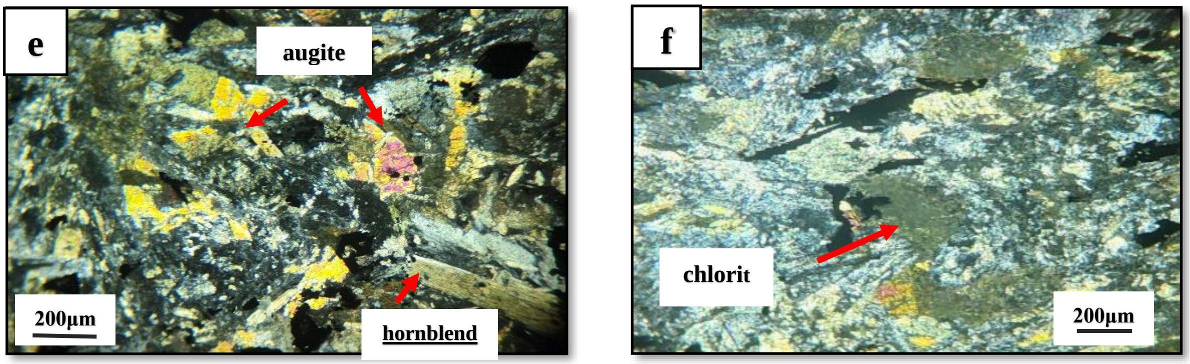

Plate 2: Photomicrographs showing the mineralogical and textural constituents of dolerite rocks (a) silicic alteration in D1[XPL], (b) sericite mineral in D2 [XPL], (c) epidote mineral in D3[XPL], (d) Anorthite in D3[XPL], (e) Hornblende and augite minerals in D4 [XPL], and chlorite minerals in D4[XPL].

2. Geochemistry

Major oxides

The major element data of the dolerite samples are listed in Table 1. The samples have a high content of SiO_2 (50.42-56.96%) with an average of 53.69%. It is obvious from Table 1 that the rocks have suffered from silicification due to hydrothermal alterations that led to an increase in silica content. There is an increase in the content of Ni and Cr with the increase of MgO content; this might be due to the crystallization of pyroxene and sometimes olivine. The separation of mafic magma occurs when magma ascends to the surface, during which olivine and pyroxene containing Ni and Cr will separate (Munyanyiwa, 1999). With the increase of MgO, the amount of Nb decreases, indicating that the magma was dry and amphibole has not crystallized. Therefore, the existence of hornblende means that hornblende in the rocks is secondary (Gardian *et al.*, 2008). According to the TAS diagram (Fig. 3), the dolerite samples are of basaltic andesite to basaltic trachy-andesite composition.

Tholeiitic and alkaline basalts can be differentiated based on their P_2O_5 levels. Tholeiitic basalts typically have lower P_2O_5 content compared to alkaline basalts (Winchester and Floyd, 1976). The behavior of the incompatible element Zr can be used along with P_2O_5 to further differentiate between tholeiitic and alkaline basalts. This is because Zr and P_2O_5 are immobile in their behavior in the magmatic differentiation. According to the different proportions of P_2O_5 contents (0.025-0.309), the dolerite rocks of Sanam salt dome fall within the alkaline and tholeiitic basalts field (Fig. 3b).

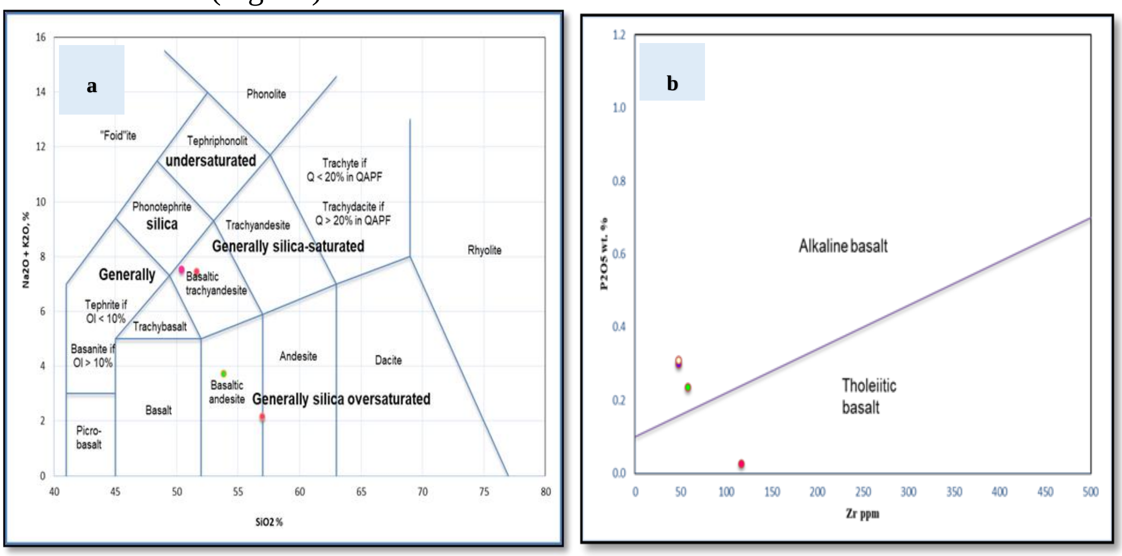

Fig. 3. a) Total alkaline vs. silica diagram (TAS diagram) (Le Bas *et al.*, 1986), b) P_2O_5/Zr classification diagram (Winchester and Floyd, 1976).

Table 1: Major oxides (in wt %) of dolerite rocks.

Sample	D1	D2	D3	D4	Min	Max	Average
SiO_2	53.83	50.42	51.62	56.96	50.42	56.96	53.69
Al_2O_3	11.28	13.82	14.31	10.26	10.26	14.31	12.285
Fe_2O_3	9.42	12.36	9.96	12.17	9.42	12.36	10.89
CaO	1.63	1.3	1.24	6.46	1.24	6.46	3.85
Na_2O	0.02	0.01	0.6	0.9	0.01	0.9	0.455
K_2O	3.7	7.5	6.85	1.27	1.27	7.5	4.385
MgO	10.78	5.25	6.89	6.5	5.25	10.78	8.015
TiO_2	2.041	2.298	2.145	1.536	1.536	2.298	1.917
MnO	0.061	0.043	0.117	0.011	0.011	0.117	0.064
P_2O_5	0.299	0.235	0.309	0.025	0.025	0.309	0.167
SO_3	0.09	0.27	0.16	0.1235	0.09	0.27	0.18
L.O. I	6.78	6.39	5.77	3.62	3.62	6.78	5.2
Total	99.931	99.896	99.971	99.835			

Trace elements

Trace element data of dolerite samples are listed in Table 2. The standard spider diagram of the trace elements normalized to primitive mantle (Fig. 4) shows an enrichment in Rb, Ta, and U, and depletion in Nb, Hf, Y, Sr, Zr, and Ba. This is due to alteration of rocks and the relative increase of other mobile elements (Yang *et al.*, 2015). The negative anomaly of Zr indicates Zr of the mantle source, as it is relatively an immobile element (Floyd and Lee, 1973; Winchester and Floyd, 1977; Macdonald *et al.*, 1988; Mir *et al.*, 2010). The low Ba concentration (26-215) ppm with a negative anomaly may indicate the lower concentration of Ba in the mantle source; also, Ba may become mobile and replace Ca due to hydrothermal activity that affected its concentration in the rocks (Smith *et al.*, 1996; Roy *et al.*, 2002). Zr, Nb, and Y are all inactive elements and are weakly affected by later alteration. The 2Nb-Zr/4-Y identification diagram (Fig. 5a) reveals a weak contamination by the crust. Two samples are located in within-plate alkali basalts and within plate tholeiitic field, one sample is located in the E-MORB field, and the other sample in the within-plate tholeiitic and island arc basalt. To determine the tectonic environment, the Hf/3-Th-Ta diagram is used (Fig. 5b), from which it is obvious that three samples fall within the alkaline field, located within-plate basalts, whereas the fourth samples fall within the E-MORB tholeiitic within-plate basalts.

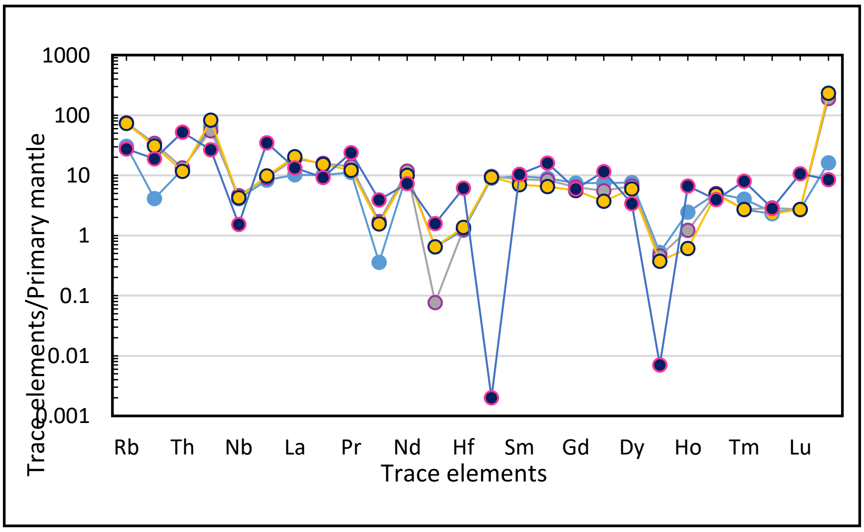

Fig. 4. Primitive mantle normalized variation spider diagram (Sun and McDonough, 1989).

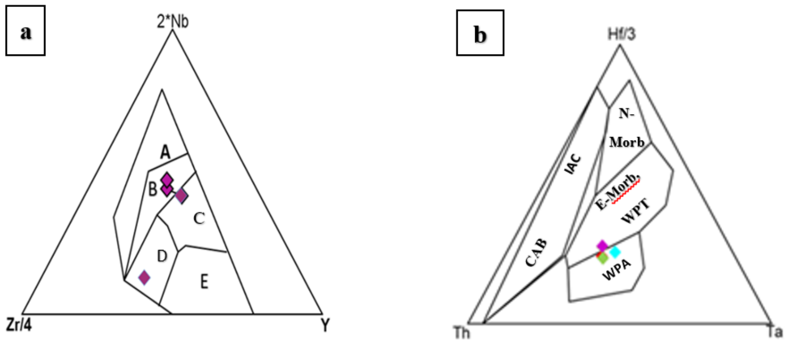

Fig. 5. a) Nb-Zr-Y discrimination diagram (A: Within-plate alkali basalts, B: Within-plate alkali basalts & within plate tholeiites, C: E-MORB enriched mid-ocean ridge basalt, D: Within-plate tholeiites basalt& island arc basalt, E: N-MORB normal mid–oceanic ridge basalt & island arc basalt (Meschede, 1986). b) Hf/3-Th-Ta diagram showing the dolerite rocks of the Sanam salt dome with respect to the fields for within –plate alkaline (WPA), within – plate tholeiitic (WPT), calc- alkaline basalt (CAB), island arc tholeiites (LAT), and normal (N)-MORB and enriched (E)- MORB (Wood, 1980).

Table 2: Trace elements of dolerite rocks (in ppm).

Sample	D1	D2	D3	D4
Zr	48	58	48	117
Hf	2.5	2.6	2.8	12.54
Ta	1.1	1.2	1.3	4.57
Nb	9.5	10.7	9.9	3.58
Th	1.5	1.6	1.4	6.25
U	3.1	2.6	3.9	1.25
Y	14.6	12.9	10.5	0.2
Rb	17	42	41	15.47
Sr	32.3	154.4	140.4	351.3
Ba	26	215	193	119.1
Sc	21.4	19.8	18.5	28.2
Cr	182	296	272	221
Co	13	20.8	24.6	70.31
Ni	57	108	93	128
Cu	24	36	53	83.5
Pb	3	35	43	1.58
Zn	38	225	228	128.6
Te	<0.5	<0.5	<0.5	2.58

Rare earth elements

The rare earth elements (REE) data of dolerite samples are listed in Table 3. REE patterns (Fig. 6) are also effective tools to understand melting degree conditions (Dervishzadeh, 1990). In most cases, low melting degrees of mantle may result in relatively isolated REE patterns, and high degrees of mantle melting may produce smooth REE patterns (Hou, 2013). Since the REE patterns of dolerite rocks are neither isolated nor completely smooth (between the two extremes), this suggests that the original magma had experienced a moderate degree of melting. REE patterns are also used to identify the crustal contamination and indications of mineralogy. Normally REE pattern of dolerites shows enrichment in LREE (Light REEs) and a smooth pattern of HREE (Heavy REEs) (Srivastava *et al.*, 2013). The dolerite rocks under study do not have such features. Therefore, they may be contaminated with crust. Rocks with the same mineralogy have similar REE patterns; the REE patterns are more or less parallel in three samples (D1, D2, D3). The low enrichment in LREE in samples indicates that these samples have suffered slight crustal contamination (Yang *et al.*, 2015). The relatively low values of Total REE may be due to the removal of LILE (large ion lithophile elements) during alteration of the studied rocks long after their replacement (Yang *et al.*, 2015). Figure (6) shows the similar patterns of the studied samples, especially with alkali basalt.

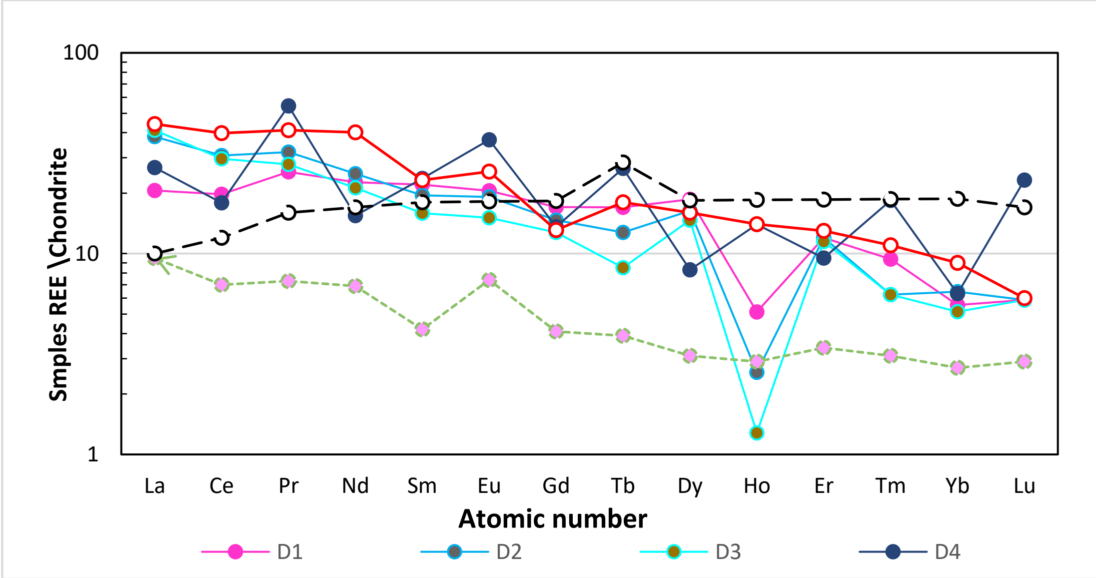

Fig. 6. Chondrite-normalized REE patterns in dolerites.

Table 3: Rare earth elements analysis of dolerite rock samples.

Element(ppm)	Sample	D1	D2	D3	D4	Min.	Max.	Avearge
LREE	La	7	13	14	9.12	7	14	10.5
	Ce	18	28	27	16.32	16.32	28	22.16
	Pr	3.09	3.88	3.37	6.58	3.09	6.58	4.835
	Nd	14.5	16	13.6	9.89	9.89	16	12.945
	Sm	4.3	3.8	3.1	4.61	3.1	4.61	3.855
	Eu	1.5	1.4	1.1	2.69	1.1	2.69	1.895
HREE	Gd	4.44	3.82	3.32	3.54	3.32	4.44	3.88
	Tb	0.8	0.6	0.4	1.25	0.4	1.25	0.825
	Dy	5.6	4.9	4.4	2.49	2.49	5.6	4.045
	Ho	0.4	0.2	0.1	1.09	0.1	1.09	0.595
	Er	2.4	2.4	2.3	1.9	1.9	2.4	2.15
	Tm	0.3	0.2	0.2	0.59	0.2	0.59	0.395
	Yb	1.22	1.42	1.13	1.39	1.13	1.42	1.275
	Lu	0.2	0.2	0.2	0.79	0.2	0.79	0.495
ΣLREE		49.39	66.08	62.17	49.21	49.21	66.08	57.645
ΣHREE		15.36	13.79	12.05	13.04	12.05	15.36	13.705
ΣLREE/ ΣLREE		3.15	4.791	5.159	3.773	3.15	5.159	4.154
ΣREE		64.75	79.87	74.22	62.25	61.26	81.44	71.035
Eu/Eu*		1.050	1.122	1.051	1.978	1.050	1.978	1.514
Ce/Ce*		0.857	0.875	0.868	0.441	0.441	0.875	0.658
$(La/Yb)_N$		3.712	5.924	8.017	4.245	3.712	8.017	5.864
$(Th/Nb)_N$		3.065	2.903	2.746	33.908	2.746	33.908	18.327
$(Nb/La)_N$		0.198	0.120	0.103	0.057	0.057	0.198	0.127
Zr/Hf		19.2	22.307	17.142	9.330	9.330	22.307	15.818
Nb/Ta		8.636	8.916	7.615	0.783	0.783	8.916	4.849

Discussion

Separation and Crystallization

It can be seen from the TAS diagram (Fig. 3a) that the four-dolerite samples are located between the sub-alkaline and alkaline series and have the characteristics of low MgO, which indicates that a certain degree of change occurred during the formation processes of the rocks, separation, and crystallization. Rare earth element analysis shows a weak positive Eu anomaly. The absence of a negative Eu anomaly in the studied samples indicates the greater activity of oxygen at the time of their appearance (Rollinson, 1993). There is negative correlation between trace elements (Ni, Cr, and V) with the mass fraction of MgO in the four-dolerite samples (Fig. 7). The mass fraction number is low, where of (Cr) is $182*10^{-6} \sim 296*10^{-6}$, Ni is $57*10^{-6}\sim128*10^{-6}$ far lower original the mass fraction (Cr) in basalt magma is $300*10^{-6}\sim650*10^{-6}$, for Ni is $295*10^{-6}\sim500*10^{-6}$, which indicates separation crystallization dominated by olivine and pyroxene during the early magmatic evolution in the dolerite samples. There is basically no correlation between the P_2O_5 mass fraction and the MgO mass fraction in the dolerite samples.

This indicates no separation and crystallization of apatite during the evolution of early magma. Therefore, the parent rock magma of the dolerite samples in the area mainly underwent separation and crystallization mainly olivine and pyroxene during the evolution processes.

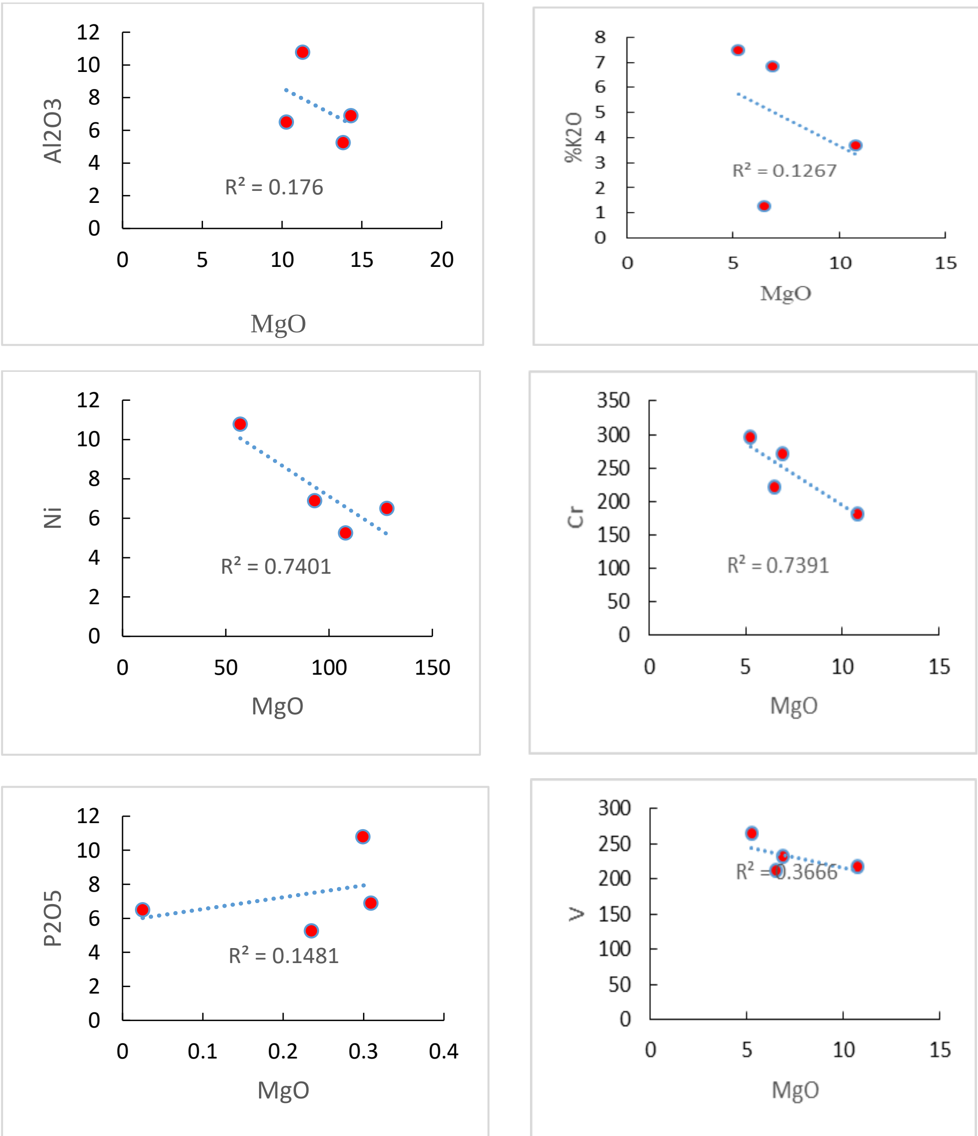

Fig. 7. Bivariate diagrams for dolerite rocks of the Sanam salt dome.

2. Crust Contamination

In continental areas, the basic magma rises from the mantle and invades the crust. During this process, varying degrees of crustal contamination will occur. Previous studies have shown that the earth crust is depleted in Nb and Ta elements and significantly enriched in La and Th elements, but the lower crust has less Th than the upper crust (Paces and Bell, 1989; Barth *et al.*, 2000). The ratio of incompatible HFSE elements is less susceptible to secondary influence of alteration and will not change over time (Xia *et al.*, 2013).

Both Th and Nb are strongly incompatible elements, and the ratio of Th/Nb is affected by the separation crystallization and can reflect the degree of magma contamination by the crust. In the study area, it is believed that during magma ascent, a contamination occurred by the crust to a certain extent, especially in sample D_4, but the intensity is not great. There are two reasons for that: first, the (Th/Nb)$_N$ values in dolerite samples are 2.746 to 33.908 with an average of 18.327 (much greater than 1). The (Nb/La)$_N$ ranges from 0.057 to 0.198 with an average of 0.127 (lower than the average in crust, 0.69), and these ratios indicate that the magma has been affected by crustal contamination. Second, the Zr/Hf values of the four dolerite samples in the study area range from 9.330 to 22.307 with an average of 15.818 (much smaller than the average in the continental crust, 33) and original mantle (CaO *et al.*, 2009). The Nb/Ta ratio of the four dolerite samples in the study area ranges from 0.783 to 8.916, with an average of 4.849 (much higher than the average of the continental crust, Nb/Ta=1), which shows a certain degree of crustal contamination during the formation processes, but the intensity was not high.

3. Magma Source

The formation of continental basalt magma is often considered the involve the lithospheric mantle. There are mainly three ways by which the lithospheric mantle participates in the formation of continental basalt magma. First, the magma originates from the partial melting of the continental lithospheric mantle (Wilson and Downes, 1991; Arndt *et al.*,1993; Qin *et al.*, 2010). Second, the magma derived from the mixing of lithospheric and asthenospheric mantle material (Hooper and Hawkesworth, 1993; Hawkesworth *et al.*,1995; Qin *et al.*, 2010). Third, the lithosphere and asthenosphere are partially melted at the same time (as the lithosphere stretches and thins, the asthenosphere gets closer to the surface, and pressure is reduced in turn, causing partial melting). Magma originating from lithospheric mantle is relatively enriched in LREE and LILE and depleted in HFSE (high-field-strength elements); whereas, if the magma originated from asthenospheric mantle, it is relatively enriched in LILE and HFSE. Within plate tholeiites have La/Yb ratios around 5-10, indicating less enrichment in LREE relative to HREE. In contrast, within-plate alkaline basalts display much higher LREE/HREE ratios, with La/Yb ratios often exceeding 20 (Macdonald *et al.*, 2001; Qin *et al.*, 2010). This significant LREE enrichment relative to HREE is a characteristic feature of within-plate alkaline magmatism, reflecting the influence of a more enriched mantle source compared to the plate tholeiites (Yildirim and Peter, 2009). Therefore, it is concluded that the present dolerite rocks are of within-plate tholeiites. The diagram in Figure 5 shows that the tectonic environment for the formation of a basic magma that introduced the studied dolerite was the WPT environment. Therefore, the dolerite magma in this case may have originated from the partial melting of the lithospheric crust and may have been contaminated by certain crustal materials during the formation processes.

The four-dolerite rocks in the study area are relatively depleted in high field strength elements (HFSE) and have characteristics of enriched mantle. The 2Nb-Zr/4-Y structural identification diagram (Fig. 5a) and the Hf/3-Th-Ta structural identification diagram (Fig. 5 b) show that the dolerite rocks were formed in a WPT environment. Since the dolerite rocks have suffered a certain degree of alteration, they have a certain impact on the chemical and mineral composition of the original rocks, which may cause certain deviations in the analysis results.

Conclusions

1- The characteristic ophitic texture dominates the dolerite rocks. The primary minerals are anorthite and clinopyroxene. Whereas, the secondary minerals are quartz, chlorite, hematite, sericite, epidote, and hornblende. The presence of sericite and chlorite is an indicator of alteration of plagioclase and pyroxene of dolerite.

2- The presence of hematite in some samples reflects the oxidization condition and high oxygen activity during later alteration processes.

3- The studied dolerite rocks are saturated and over-saturated basalt type and range in composition from basaltic andesite to basaltic trachyandesite and fall within the alkaline and tholeiitic basalt fields. L.O.I values indicate that these dolerites have been affected by low-grade hydrothermal alteration and weathering processes.

4- The slightly positive Eu anomaly indicates the oxidation environment. Based on Eu and REE behavior, there is a similarity between the studied dolerite and alkaline basalt.

5- The pattern of REE in the studied dolerite rocks, combined with the chemical analyses suggests that the present dolerite rocks are of within-plate tholeiites.

Reference

Al- Naqib, K.M., 1970. Geology of Jabal Sanam, South Iraq. Jour. Geol. Soc. Iraq, Vol. 3, No. 1, pp. 9-36.

Al-Ali, S., Hannina, S., Soltan, B., Vartanian, K. and Rukes, K., 2022. Natural Radioactivity and its Hazards of Infracambrain Rocks at Jabal Sanam Structure, Southern Iraq. Iraqi Journal of Science, Vol. 63, No. 12, pp. 5386-5401. DOI: https://doi.org/10.24996/ijs.2022.63.12.25.

Al-Ali, S. and Al-Khafaji, S.J., 2023. Spatial distribution and reserve estimation of sand and gravel deposits using geostatistical methods in West Basrsh, southern Iraq. Kuwait Journal of Science, Vol. 50, pp. 127-137. https://doi.org/10.1016/j.kjs.2023.02.017

Al-Bassam, K.S., 2011. Petrology and chemistry of some exotic rock fragments from Jabal Sanam, Basrah, Iraq. Iraqi Bulletin of Geology and Mining, Vol. 7, p. 39-53.

Al-Mudhafar, Z.Q. and Al-Mashaikie, S.Z., 2019. Petrology of the rock sequence at Jabal Sanam in Basrah, southern Iraq. Unpublished MSc Thesis, Babylon University, pp 69.

Al-Muttory, W.K., 2002. Structure and tectonism of Jabal Sanam, Southern Iraq. Unpublished MSc Thesis, Basrah University, 93 pp. (in Arabic).

Arndt, N.T., Czamanske, G.K., Wooden, J.L., *et al.*, 1993. Mantle and Crustal Contributions to Continental Flood Volcanism. [J]. Tectonophysics, 1993,223(1/2):39-52. https://doi.org/10.1016/0040-1951(93)90156-E.

Barth, M.G., Mcdonough, W.F., Rudnick, R. L., 2000.Tracking the Budget of Nb and Ta in the Continental Crust[J]. Chemical Geology, 165(3/4): 197-213. DOI: 10.1016/S0009-2541(99)00173-4

Billings, M.P., 1972. Structural Geology. 3rd. ed., New Delhi Prentice-Hall, Inc., P. 606.

Buday, T. and Jassim, S.Z., 1987. The Regional Geology of Iraq: Vol. 2, Tectonism, Magmatism and Metamorphism. S.E. Geological Survey and Mineral Investigation, Baghdad, Iraq, 352 P.

CaO, Jianjin., Hu, Ruizhong., Xie, Guiqing., 2009. Geochemistry and Genesis of Mamic Dikes from the Coastal Area of Guangdong Province, China [J]. Acta Petrologica Sinica, 25 (4): 9841000.

Dervishzadeh A., 1990. Geological features of the Persian Gulf Infracambrian salts, Collection articles of Diapirism symposium with a Special approach to Iran, first Cover. Floyd, P.A. and Less, G.J. (1973) Ti-Zr characterization of some Cornish pillow lavas. Proc. Ussher Soc. 2, pp. 489-494.

Floyd, P.A. and Winchester, J.A., 1975. Magma type and tectonic setting discrimination using immobile elements: Earth and Planetary Science Letters, Vol. 27, pp. 211-218. https://doi.org/10.1016/0012-821X(75)90031-X.

Frost, B.R. and Frost, C.D., 2008. A geochemical classification for feldspathic igneous rocks. Journal of Petrology, v. 49, p. 1955-1969. https://doi.org/10.1093/petrology/egn054.

Gardien, V., Lecuyer, C., Moyen, J.F., 2008. "Dolerite of the Woodlark Basin (Papuan Peninsul, New Guinea); A geochemical record of the influence of a neighboring subduction zone", Journal of Asian Earth Sciences 33139-154. DOI: 10.1016/j.jseaes.2007.12.003.

Hawkesworth, C., Turner, S., Gallagher, K., *et al.*, 1995. Calc-Alkaline Magmatism, Lithospheric Thinning and Extension in the Basin and Range[J]. Journal of Geophysical Research: Solid Earth, 100(6): 1027110286.

Hooper, P.R., Hawkesworth, C.J., 1993. Isotopic and Geochemical Constraints on the Origin and Evolution of the Columbia River Basalt[J]. Journal of Petrology, 6(6): 12031246. https://doi.org/10.1093/petrology/34.6.1203.

Hou T., Zhang Z., Santosh M., Encarnacion J., Wang M., 2013. The Cihai diabase in the Beishan region, NW China: Isotope geochronology, geochemistry and implications for Cornwall-style iron mineralization, Journal of Asian Earth Sciences, 70-71, pp. 231-249. http://dx.doi.org/10.1016/j.jseaes.2013.03.016.

LeBas, M.J., Le Maitre, R.W., Streckeisen, A. and Zanettin, B., 1986. A chemical classification of volcanic rocks based on the total alkali-silica diagram: Journal of Petrology, Vol. 27, pp. 745-750. https://doi.org/10.1093/petrology/27.3.745.

LeMaitre. R.W., Bateman, P., Dudek, A., Keller, J., Lameyre, J. Le Bas, M.J., Sabine, P.A., Schmid, R., Sorensen, H., Streckeisen, A., Woolley, A.R. & Zanettin, B., 1989. A Classification of Igneous Rocks and Glossary of Terms: Recommendations of the International Union of Geological Sciences Subcommission on the Systematics of Igneous Rocks. Blackwell Scientific Publications, Oxford, U.K.

Macdonald, R., Millward, D., Beddoe-Stephens, B. and Layborn-Parry, J., 1988. The role of tholeiitic magmatism in English Lake District: Evidence from dyke in Eskdace. Min. Mag. 52, pp. 459-472. https://doi.org/10.1180/minmag.1988.052.367.04.

Macdonald, R., Rogers, N.W., Fitton, J.G., *et al.*, 2001. Plume Lithosphere Interactions in the Generation of the Basalts of the Kenya Rift, East Africa[J]. Journal of Petrology, 42(5): 877900. https://doi.org/10.1093/petrology/42.5.877.

Meschede, M., 1986. A method of discriminating between different types of mid-ocean ridge basalts and continental tholeiites with the Nb-Zr-Y diagram: Chemical Geology, v. 56, pp. 207-218. https://doi.org/10.1016/0009-2541(86)90004-5.

Mir, A.R., Alvi, S.H. and Balaram, V., 2010. Geochemistry of mafic dikes in the Singhbhum Orissa craton: implications for subduction-related metasomatism of the mantle beneath the eastern Indian craton. Int. Geol. Rev. 52, pp. 79-94. https://doi.org/10.1080/00206810903211948.

Munyanyiwa, H., 1999. Geochemical study of the Umkondo dolerite and lavas in the Chimanimani and Chipinge Districts (eastern Zimbabwe) and their regional implications", Journal of African Earth Science 26(2), pp. 349-365.

Paces, J.B., and Bell, K., 1989. Non-Depleted Subcontinental Mantle Beneath the Superior Province the Canadian Shield: Nd -Sr Isotopic and Trace Element Evidence from Midcontinent Rift Basalts [J]. Geochemicaet Cosmochimica Acta, 53(8):2023,2035.

Qin Shecai., Fan Weiming., Guo Feng, *et al.*, 2010. Petrogenesis of Late Mesozoic Diabase Dikes in Zhejiang Fujian Provinces: Constraints from AR-AR dating and geochemistry. 26(11):3295-3306.

Roy, A., Sarkar, A., Jeyakumar, S., Aggrawal, S.K. and Ebinhara, M., 2002. Sm-Nd age and mantle source characteristics of the Dhanjori volcanic rocks, Eastern India. Geochem. J. 36, 503-518. https://doi.org/10.2343/geochemj.36.503.

Rollinson, H., 1993. Using geochemical data: Evaluation, Presentation, Interpretation. Singapore Longman. https://doi.org/10.1016/0098-3004(95)90001-2.

Rogers, N.W., 1992. Potassic magmatism as a key to trace element enrichment processes in the upper mantle. Journal of Volcanology and Geothermal Research 50: pp. 85-99.

Rudnick, R. L., Fountain, D. M., 1995. Nature and Composition of the Continental Crust: A Lower Crustal Perspective[J] Reviews of Geophysics, 33(3):267. http://dx.doi.org/10.1029/95RG01302.

Smith, T.E., Thirwall, M.F. and Macpherson, C., 1996. Trace element and isotope geochemistry of volcanic rocks of Bequia, Grenadine Islands, Lesser Antilles arc: a study of subduction enrichments and intra-crustal contamination. J. petrol. 37, pp. 117-143. https://doi.org/10.1093/petrology/37.1.117.

Soltan, B.H., 2002. Petrology and Origin of Jabal Sanam Structure, Southern Iraq. Unpublished MSc Thesis, Basrah University, 86 P. (in Arabic).

Soltan, B.H., 2020. Petrology and stratigraphy of Pre-Cambrian Hormuz Series outcrop in Jabal Sanam structure –the oldest surface rocks in Iraq. Basrah Journal of Science, Vol. 38(3), pp. 497-520. http://basjsci.net/index.php/bsj/article/view/33/24.

Srivastava, R.K., Jayananda, M., Gautam. G. C., Gireesh, V., Samal, A.K., 2013. "Geochemistry of an ENE–WSW to NE–SW trending ~2.37 Ga mafic dyke swarm of the eastern Dharwar craton, India.

Sun, S.S. and McDonough, W.F., 1989. Chemical and isotopic Systematics of Oceanic Basalts: Implications for mantle Composition and processes. Geological Society London Special Publications, 42, pp. 313-345. http://dx.doi.org/10.1144/GSL.SP.1989.042.01.19.

Wang, K. and Davis, E.E., 2003. High permeability of Young Oceanic Crust Constrained by Thermal and Pressure Observations (in Land and Marine Hydrogeology), pages 165-188. http://dx.doi.org/10.1016/B978-044451479-0/50023-6.

Wang, Y., Chung, S., Oreilly, L., Sun, S. Y., Shinjo, R., Chen, C.H., 2004. Geochemical constration for the genesis of post-collisional magmatism and geodynamic evolution of the Northen Taiwan region. Journal of Petrology 45: pp. 975-1011. http://dx.doi.org/10.1093/petrology/egh001.

Winchester, J.A. and Floyd, P.A., 1977.Geochemical discrimination of different magma series and their differentiation products using immobile elements. Chemical Geology 20, pp. 325-343.

Winchester, J.A. and Floyd, P.A., 1976. Geochemical magma type discrimination: application to altered and metamorphosed basic igneous rocks. Earth and Planetary Science Letters, 28, pp. 459-469. https://doi.org/10.1016/0012-821X(76)90207-7.

Wilson, M. and Downes, H., 1991. Tertiary-Quaternary Extension-Related Alkaline Magmatism in Western and Central Europe[J]. Journal of Petrology, 32 (4): pp. 811-849. https://doi.org/10.1093/petrology/32.4.811.

Wood, D.A., 1980, The application of a Th-Hf-Ta diagram to problems of tectonomagmatic classification and to establishing the nature of crustal contamination of basaltic lavas on the British Tertiary Volcanic Province: Earth and Planetary Science Letters, Vol. 50, pp. 11-30. https://doi.org/10.1016/0012-821X(80)90116-8.

Xia, Linyin., Xia, Zuchun., Xu, Xueyi., *et al.*, 2013. Intracontinental Volcanism in Central and Western China and Its Adjacent Areas[M]. Beijing: Science Press.

Yildirim D. and Peter Thy, 2009. Island arc tholeiite to boninitic melt evolution of the Cretaceous Kizildag (Turkey) ophiolite: Model for multi-stage early arc–forearc magmatism in Tethyan subduction factories. Lithos 113(1-2): pp. 68-87. http://dx.doi.org/10.1016/j.lithos.2009.05.044.

Yang, X., Zhang, Z., Guo, S., Chen, J., Wang, D., 2015. Geochronological and geochemical studies of the metasedimentary rocks and diabase from the Jingtieshan deposit, north Qilian, NW China: Constraints on the associated banded iron formation. Ore Geology Reviews. https://doi.org/10.1016/j.oregeorev.2015.10.018.